# Reliability Assessment of Power Supply Systems Integrated with Renewables for Electric Road System

Wei Zuo, Kang Li, and Jihai Zhong

*Abstract*—**With the rapid expansion of urban road networks and the increasing ownership of vehicles in many countries and regions, the greenhouse gas and pollutant emissions from road travels have become a global concern. The introduction of electric vehicles (EVs) with dynamic charging into road systems, which is defined as electric road systems (ERSs), has been widely recognized as a viable solution to address this problem. This paper presents a comprehensive study on the reliability of power supply systems integrated with renewables for ERS (ERS-PSRs), which interface with both road traffic and power networks. First, a brief introduction to the charging modes of EVs demonstrates the coupling of the two networks. A simplified traffic model is then built, based on which the reliability indices of the system considering the influence of the dynamic charging and static charging modes of EVs are proposed. Further, a simplified trip chain based Monte Carlo reliability assessment method of ERS-PSRs is proposed. Case studies based on the IEEE Roy Billinton Test System (RBTS) show that the dynamic charging mode of EVs can not only effectively balance the supply and demand of the power grid at different time (shaving peaks and filling valleys), but also significantly improve the reliability of ERS-PSRs. The case studies also examine the effects of the ratio of EVs with dynamic charging, wind generation penetration rate, additional wind power, and battery energy storage systems (BESSs) on the reliability of ERS-PSRs.**

*Index Terms*—**Electric road system (ERS), electric vehicle, dynamic charging mode, renewable energy, reliability, power supply.**

## I. Introduction

OVER the past few decades, the ownership of vehicles has steadily increased in many countries and regions along with the global industrialization and urbanization, leading to increasing concerns on the consequent energy and environmental problems. The high consumption of fossil fuels in the transportation sector has made it one of the largest contributors to greenhouse gas emissions, which drive the global climate change and environment pollution [1], [2]. As of 2022, about 30% of railway lines around the world have been electrified, which accounts for approximately 1.9% of the total energy demand and 1.2% of carbon emissions in the transportation sector [3]. In contrast, the road systems account for about 75% of the total energy consumption and approximately 76.6% of carbon emissions in the transportation sector, which is significantly higher than the rail system [4]. To address these issues, electric vehicles (EVs) and renewable energy have become the focus of low-carbon technology development [5]. In response to the net-zero targets set by many governments, the automotive industry has invested heavily in the development of low-carbon and clean-energy vehicles such as plug-in EVs. For example, in the UK, the plug-in EVs accounted for a record-breaking number of more than 16.3% of new vehicle registrations in 2021, with pure battery electric vehicles (BEVs) making up 11.1% [6]. Additionally, China sold about 3.3 million EVs in 2021, which represents a greater number than the total sales worldwide in 2020, and Europe also demonstrated a notable increase in EV sales, accounting for up to one-third of the global sales [7].

Although the introduction of EVs offers a tangible solution for the decarbonization of transportation, it remains unclear whether EVs can entirely replace fossil fuel-powered vehicles, in particular for heavy-goods EVs (HEVs). At present, the refueling process of the fossil fuel-powered vehicles requires only 3-5 min, while EVs require a longer charging time of several hours [8]. In order to overcome these limitations, the electric road system (ERS) combining static and dynamic charging modes are considered to be a viable alternative solution to the decarbonization of transportation [2], [9], [10]. The ERS is a road system that supplies electric power to vehicles travelling on it through three different technologies, namely overhead lines, conductive rail, and inductive/wireless rail [11]-[13]. Meanwhile, for both the ERS and other traditional transportation systems, their traction power supply systems (TPSSs), such as metros or railways, share the common objectives of providing electric power to moving vehicles. However, different from overhead line and conductive rail based ERSs, the inductive/wireless rail based ERS has its own specific dynamic charging mode for EVs. In comparison to railways and metros, the traction load demands of ERS are more stochastic. This is due to the fact

Manuscript received: October 9, 2023; revised: February 10, 2024; accepted: June 26, 2024. Date of CrossCheck: June 26, 2024. Date of online publication: August 7, 2024.

This work was supported by the China Scholarship Council (No. 202006130002).



W. Zuo (corresponding author), K. Li, and J. Zhong are with the School of Electronic and Electrical Engineering, University of Leeds, Leeds, UK (e-mail: elwz@leeds.ac.uk; K.Li1@leeds.ac.uk; ml18j34z@leeds.ac.uk).

DOI: 10.35833/MPCE.2023.000769

that the load demands of railways and metros are scheduled and thus more predictable, while those of ERS are influenced by many factors such as vehicle types, drivers' behaviors, and weather. Accordingly, to address the reliability assessment of power supply systems for ERS, a principal objective of this paper is to establish a new load model that incorporates the static and dynamic charging modes of EVs. This paper focuses on the inductive/wireless rail based ERS, which uses induction devices to transmit electricity from the road to EV through the electromagnetic induction. While the majority of ERSs are still at the experimental phase, the OLEV project in South Korea and the Smartroad Gotland project in Sweden have demonstrated promising outcomes [14], [15].

In the energy and power sector, the proportion of renewable energy such as wind energy in the power grid is increasing to address the climate challenge due to substantial greenhouse gas emissions from thermal power plants [16]. To further reduce the wind power forecasting errors, the risk-based evaluation methods are proposed [17]. This paper considers a future ERS by integrating renewable energy with its power supply system and then examines its operational reliability. The proposed reliability assessment of power supply system integrated with renewables for ERS (ERS-PSRs) focuses on the new load model including the static and dynamic charging modes of EVs. To fully assess the impact of the EV deployment, the wind power and battery energy storage system (BESS) are integrated with the power supply system of ERS.

To investigate the impact of dynamic charging and renewables on the reliability assessment, it is crucial to model the traffic patterns and power system. ERS-PSR is a new area, and little has been done so far. Nevertheless, extensive studies have been conducted on renewable generation technologies and the interaction effects of EVs with power grid [2]. For example, [18] and [19] introduce some reliability indices and analysis methods of the TPSSs for electrified railway, which can be applied to ERSs. Reference [20] proposes a set of resilience enhancement strategies, including line hardening and the placement of distributed generators, for the power distribution network coupled with urban transportation system, which would be beneficial to improving the overall system reliability. References [21]-[23] develop and validate an autoregressive moving average (ARMA) model for wind speed prediction, while [24] and [25] propose several forecasting models for wind power generation based on wind speed. The models for EV charging are introduced in [26] and [27]. The ERS-PSR offers the dynamic charging to electrify the on-road EVs including HEVs. However, no suitable evaluation method has yet been proposed to assess its reliability. This paper bridges this research gap by proposing a set of reliability indices for the ERS-PSRs and a time-series daily trip chain based Monte Carlo reliability assessment method is proposed.

The remainder of this paper is organized as follows. Section II presents the charging modes and daily trip chains of EVs in ERS-PSRs. Section III gives the detail of the power interaction model of ERS-PSRs. Section IV introduces several reliability indices and the trip chain based Monte Carlo reliability assessment method for ERS-PSRs. The case studies are presented in Section V, where the simulation results are detailed. Finally, Section VI concludes this paper.

## II. Charging Modes and Daily Trip Chains of EVs in ERS-PSRs

The introduction of the dynamic charging has a significant impact on the existing EV charging market. The charging mode and trip trains of EVs in ERS-PSRs are discussed in detail below.

### *A. Charging Modes of EVs*

In ERS-PSRs, both dynamic and static charging modes of EVs are considered, where EVs can be charged at various charging points along the daily travel trajectory or be charged while driving, thus ensuring that EVs can travel longer distances without concerns on insufficient battery capacity. For the static charging, the charging stations are often situated in densely-populated urban areas and along strategic road routes with high charging demand. In contrast, the dynamic charging focuses on the wireless charging through the reequipped chargeable road sections. Consequently, the charging modes of EVs in ERS-PSRs mainly include conventional plug-in, fast plug-in, and static and dynamic wireless charging options. Their advantages and disadvantages are summarized as follows.

1) Conventional plug-in charging: it has a relatively low charging power and requires a long charging time, which is unsuitable for EVs on travel. Nevertheless, its installation cost is low, and the charging management can be more flexible.

2) Fast plug-in charging: it has a higher charging power and much shorter charging time (e. g., 20 min to 1 hour), which is often used for EVs on travel.

3) Static wireless charging: it eliminates the mechanical charging interface and EVs only need to be parked in the designated parking space, which is simple and convenient without additional operations. However, its low charging efficiency and other technical and environmental factors limit its application.

4) Dynamic wireless charging: as a new charging technology, it employs the wireless induction technology to facilitate charging for EVs on roads. The elimination of physical connections such as power cords and sockets, makes charging more accessible and straightforward. However, the associated road reconstruction and maintenance costs are relatively high.

### *B. Daily Trip Chains of EVs*

The typical daily travel trajectory of EVs often encompasses a few locations, including home, work place/school, shopping/leisure places, and other places. It is often assumed that the charging facilities are installed at these locations, and the travel plan of EVs comprises two distinct phases: charging when parked and consuming when in motion [11], [28]. However, the travel trajectory of EVs in ERS-PSRs has an additional charging point, known as dynamic charging road. The trip chain model can be used to simulate the travel trajectory of EVs in a wider context, as discussed in [29]. The trip chains of EVs in the traditional road system and ERS-PSRs, taking into account various charging points, are detailed in Table I, where the ratios $R$ with different subscripts are the proportions of EVs in the corresponding trip chains to the total number of EVs.

TABLE I
TRIP CHAINS OF EVS IN TRADITIONAL ROAD SYSTEM AND ERS-PSRS

| Type | No. | Trip chain | Ratio |
|---|---|---|---|
| Traditional road system | A1 | $H\rightarrow W\rightarrow H$ | $R_1$ |
| | A2 | $H\rightarrow W\rightarrow S(O)\rightarrow H$ | $R_2$ |
| | A3 | $H\rightarrow S(O)\rightarrow H$ | $R_3$ |
| ERS-PSR | B1 | $H\rightarrow W\rightarrow H$ | $R_{11}$ |
| | B2 | $H\rightarrow D\rightarrow W\rightarrow D\rightarrow H$ | $R_{12}$ |
| | B3 | $H\rightarrow W\rightarrow S(O)\rightarrow H$ | $R_{21}$ |
| | B4 | $H\rightarrow D\rightarrow W\rightarrow D\rightarrow S(O)\rightarrow D\rightarrow H$ | $R_{22}$ |
| | B5 | $H\rightarrow S(O)\rightarrow H$ | $R_{31}$ |
| | B6 | $H\rightarrow S(O)\rightarrow D\rightarrow H$ | $R_{32}$ |

Note: H represents home; W represents workplace/school; S represents shopping/leisure places; D represents dynamic charging road; and O represents other places.

In both traditional road system and ERS-PSRs, the trip chains of most EVs, particularly passenger vehicles, have the same origin and destination, i. e., home. This suggests that most EVs leave home in the morning and return home at night, while their daily travel trajectory cover several fixed locations. As illustrated in Table I, the typical trip chains A1-A3 do not encompass dynamic charging roads. The introduction of dynamic charging gives rise to significant changes in the trip chains. To illustrate, chain A1 is divided into chains B1 and B2 with different ratios. The ratios in Table I satisfy:

$$R_1+R_2+R_3=1 \tag{1}$$

$$\begin{cases} R_{11}+R_{11}=R_1 \\ R_{21}+R_{21}=R_2 \\ R_{31}+R_{31}=R_3 \end{cases} \tag{2}$$

Besides, each trip chain has its own trip segments. Taking chain B2 as an example, the chain B2 can be described as:

$$C_{\mathrm{B2}}=C_{\mathrm{H}\rightarrow \mathrm{D}}+C_{\mathrm{D}\rightarrow \mathrm{W}}+C_{\mathrm{W}\rightarrow \mathrm{D}}+C_{\mathrm{D}\rightarrow \mathrm{H}} \tag{3}$$

where $C$ represents the trip chain segments.

## III. POWER INTERACTION MODEL OF ERS-PSRS

In addition to the benefits of dynamic charging, another advantage is the integration of renewable energy (wind power), which can not only alleviate the pressure of supplying additional load but also reduce the emission of carbon dioxide. However, the uncertainty of renewable energy (variable wind speed and various operation states) and the variable load demand may introduce significant but unknown reliability impacts on the power system. To investigate such reliability impacts, this section will investigate the modelling of the ERS-PSRs, where EVs are treated as pure loads.

### A. Load Model of EVs

Loads of EV in the ERS depend on various factors including environmental, infrastructural, technical, and market-related aspects. This paper primarily addresses the technical aspects of load model for EVs. The daily charging schedule for EVs considered in this paper includes three options, i.e., charging once, twice, and three times per day, and it is assumed that each option includes a certain ratio of EVs with dynamic charging. Therefore, the charging load and charging time can be estimated according to the difference in battery capacity at different time. It is assumed that the state of charge (SoC) of an EV is 100% when it leaves home and there are a total of $N$ EVs. The daily charging demand of each EV, also known as the load model of EV at time $t$, can be defined as:

$$SoC_{i,t+1}=SoC_{i,t}+\alpha_c P_c T_c/(60\cdot EH) \tag{4}$$

$$P_c=\begin{cases} P_{cm1} & \text{conventional plug - in charging} \\ P_{cm2} & \text{fast plug - in charging} \\ P_{cd} & \text{dynamic charging} \end{cases} \tag{5}$$

where $SoC_{i,t}$ is the battery SoC of the $i^{\text{th}}$ EV at time $t$; $\alpha_c$ is the charging efficiency; $P_c$ is the rated charging power of EV in different charging modes, and the subscripts $m1$, $m2$, and $d$ correspond to the conventional plug-in charging, fast plug-in charging, and dynamic charging modes, respectively [30]; $T_c$ is the charging time (min); and $EH$ is the rated battery capacity of EVs (kWh).

When $SoC_{i,t+1}-SoC_{i,t}>0$, the charging time $T_c$ can be obtained by (6); otherwise, $T_c=0$.

$$T_c=\left(SoC_{i,t+1}-SoC_{i,t}\right)\cdot EH\cdot 60/\left(\alpha_c P_c\right) \tag{6}$$

Therefore, the load power of all EVs in ERS-PSRs at time $t$ is denoted as $P_{EV,cha,t}$, which can be obtained by:

$$P_{EV,cha,t}=\sum_{i\in\Omega_{EV,cha}} P_{cm1,i,t}+P_{cm2,i,t}+P_{cd,i,t} \tag{7}$$

$$\Omega_{EV,cha}=\left\{i \mid 0<\varpi_i<100\%\right\} \tag{8}$$

where $\Omega_{EV,cha}$ is the set of EVs with their separate SoC values; and $\varpi_i$ is the SoC value of the $i^{\text{th}}$ EV.

### B. Model of Wind Power Generation

Suppose the wind power is integrated with the ERS. The randomness of wind speed results in variable wind power generation. It is therefore essential to develop models for predicting the wind power. In some regions, a time-series ARMA model is usually chosen to predict the wind speed, as given in (9). Then, based on the predicted wind speed, the polynomial power function (PPF) can be applied to calculate the wind power generation [22], [31].

$$Y_t=\sum_{k=1}^{p} a_k Y_{t-k}+\sum_{j=1}^{q} b_j e_{t-j} \tag{9}$$

where $Y_t$ is the predicted wind speed at time $t$; $Y_{t-k}$ is the actual wind speed at time $t-k$; $e_{t-j}$ is the disturbance erm; $a_k$ and $b_j$ are the coefficients; and $p$ and $q$ are the orders of this model.

According to the principle of wind power generation, only when the actual wind speed reaches the cut-in speed will the wind turbines start to generate electricity [32]. Conversely, the wind turbines cease to generate electricity when the actual wind speed exceeds the cut-out wind speed [33]. For the $i^{\text{th}}$ wind power generator at time $t$, the relationship between its generated wind power $P_{w,i,t}$ and the wind speed $V_{w,i,t}$ can be illustrated in Fig. 1.

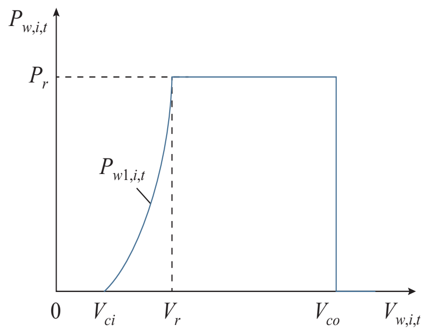


Fig. 1. Generated wind power with different wind speeds.

As can be observed, the generated wind power stays at the rated power $P_r$ only when the wind speed is between the rated wind speed $V_r$ and the cut-out wind speed $V_{co}$. Besides, when the wind speed exceeds the cut-in speed $V_{ci}$ but is lower than the rated wind speed $V_r$, the generated wind power varies with the wind speed.

The generated wind power can be expressed as:

$$P_{w,i,t}=\begin{cases}0 & V_{w,i,t}\leq V_{ci} \text{ or } V_{co}<V_{w,i,t}\\ P_{w1,i,t} & V_{ci}<V_{w,i,t}<V_r\\ P_r & V_r\leq V_{w,i,t}\leq V_{co}\end{cases} \tag{10}$$

where $P_{w1,i,t}$ is the non-linear part of generated wind power when $V_{ci}<V_{w,i,t}<V_r$, which is calculated using polynomial [24], [34] as:

$$P_{w1,i,t}=C_1+C_2V_{w,i,t}+C_3V_{w,i,t}^2 \tag{11}$$

$$C_1=C_0\left[V_{ci}\left(V_{ci}+V_r\right)-4V_{ci}V_r\left(\frac{V_{ci}+V_r}{2V_r}\right)^3\right] \tag{12}$$

$$C_2=C_0\left[4\left(V_{ci}+V_r\right)\left(\frac{V_{ci}+V_r}{2V_r}\right)^3-3V_{ci}-V_r\right] \tag{13}$$

$$C_3=C_0\left[2-4\left(\frac{V_{ci}+V_r}{2V_r}\right)^3\right] \tag{14}$$

$$C_0=\frac{1}{\left(V_{ci}-V_r\right)^2} \tag{15}$$

Therefore, the total generated wind power at time $t$ $P_{w,t}$ can be calculated as:

$$P_{w,t}=\sum_{i=1}^{N_w}P_{w,i,t} \tag{16}$$

where $N_w$ is the number of wind power generators.

### C. Operating States of Power Sources in ERS-PSRs

The power sources of ERS-PSRs usually include the thermal power plants and renewable energy sources such as wind power generators, where the former is conventionally utilized to cover the base load, and the latter can be utilized to cover the additional demand from flexible loads such as EVs. The operating states of these power sources differ slightly based on their roles.

#### 1) Operating States of Thermal Power Plants

For the thermal power plants, the operating states can be classified into up and down states, which can be described as the normal and failed states, respectively. The two-state model for thermal power plants and its state curves are illustrated in Fig. 2(a) and (b), respectively, where *TTF* and *TTR* are the operating time and repair time, respectively; and *MTTF* and *MTTR* are the mean values of *TTF* and *TTR*, respectively, which are obtained through random sampling. It is always assumed that the operating time and repair time obey the exponential distribution [2].

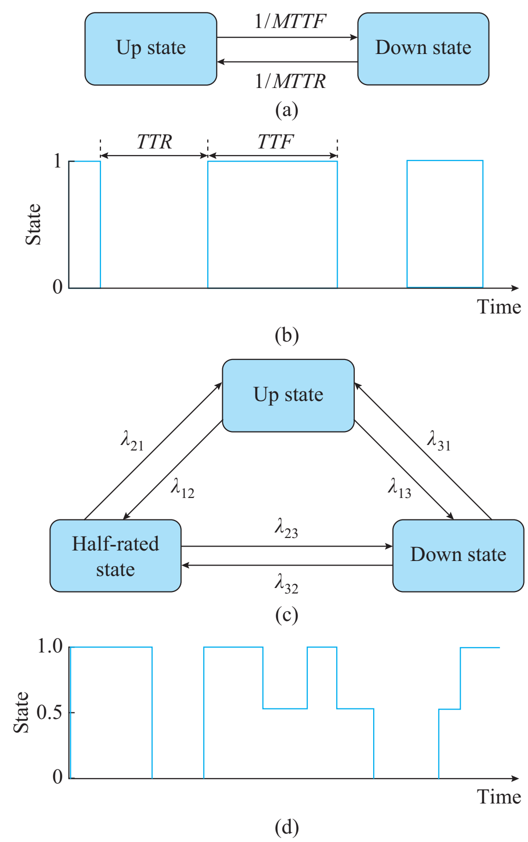


Fig. 2. State models and curves for power sources. (a) Two-state model for thermal power plants. (b) State curve of two-state model. (c) Three-state model for wind power generator. (d) State curve of three-state model.

As shown in Fig. 2(b), the thermal power plants alternate between the up and down states, of which the durations can be calculated as:

$$T_{up}=-MTTF\cdot\ln U \tag{17}$$

$$T_{down}=-MTTR\cdot\ln U' \tag{18}$$

where $T_{up}$ and $T_{down}$ are the durations of the up and down states, respectively; and $U$ and $U'$ are the random numbers between 0 and 1.

Once the duration of each state is obtained, the total generated power of thermal power plants at time $t$ $P_{g,t}$ can be expressed as:

$$P_{g,t}=\sum_{i=1}^{N_g}P_{g,i,t}S_{g,i,t} \tag{19}$$

$$S_{g,i,t}=\begin{cases}1 & \delta<p_{up\to down}\\ 0 & \delta<p_{down\to up}\end{cases} \tag{20}$$

where $S_{g,i,t}$ is the operating state of the $i^{\text{th}}$ thermal power plant at time $t$, which equals 1 in the up state and 0 vice versa; $P_{g,i,t}$ is the generated power of the $i^{\text{th}}$ thermal power plant at time $t$; $p$ is the state transition probability between different states; the subscripts *up* and *down* denote the up and down states, respectively; $\delta$ is the state transition probability at time $t$ between up and down states; and $N_g$ is the number of thermal power plants.

*2) Operating States of Wind Power Generators*

For the wind power generators, the operating state is simulated by using a three-state model, as shown in Fig. 2(c). Similar to the two-state model, the up and down states represent the normal and failed states, respectively. In addition, in the cases where the full output power cannot be supplied, the half-rated state with a state value of 0.5 is defined, as illustrated in Fig. 2(d). Meanwhile, the duration of each state in the three-state model, i. e., $T_{up}$, $T_{de}$, and $T_{do}$, can be achieved by (21)-(23), respectively. Furthermore, the power generated by the wind power generator at time $t$ can be calculated using (24).

$$T_{up}=\min\left(-\frac{1}{\lambda_{12}}\ln U_1,-\frac{1}{\lambda_{13}}\ln U_2\right) \tag{21}$$

$$T_{de}=\min\left(-\frac{1}{\lambda_{21}}\ln U_3,-\frac{1}{\lambda_{23}}\ln U_4\right) \tag{22}$$

$$T_{do}=\min\left(-\frac{1}{\lambda_{31}}\ln U_5,-\frac{1}{\lambda_{32}}\ln U_6\right) \tag{23}$$

$$P_{w,t}=\sum_{w=1}^{N_w}P_{w,i,t}S_{w,i,t} \tag{24}$$

$$S_{w,i,t}=\begin{cases}0 & \delta<p_{do\to up}+p_{do\to de}\\ 0.5 & \delta<p_{up\to de}+p_{do\to de}\\ 1 & \delta<p_{up\to do}+p_{up\to de}\end{cases} \tag{25}$$

where $U_1$-$U_6$ are the random numbers between 0 and 1; $\lambda_{12}$, $\lambda_{13}$, $\lambda_{21}$, $\lambda_{23}$, $\lambda_{31}$, and $\lambda_{32}$ are the failure rates of different states; $S_{w,i,t}$ is the operating state of the $i^{\text{th}}$ wind power generator at time $t$; and the subscript *do* denotes the half-rated state.

Therefore, the total generated power of ERS-PSRs $P_{G,t}$ is calculated as:

$$P_{G,t}=P_{g,t}+P_{w,t}=\sum_{i=1}^{N_g}P_{g,i,t}S_{g,i,t}+\sum_{i=1}^{N_w}P_{w,i,t}S_{w,i,t} \tag{26}$$

## IV. Trip Chain Based Monte Carlo Reliability Assessment Method for ERS-PSRs

The deployment of a large number of EVs introduces a significant amount of load to the power grid [11]. With the dynamic charging mode of EVs, the issue of extra load demands becomes more severe, while the electric roads have the potential to alleviate the mileage limitation due to limited battery capacity and the charging pressure during peak hours. The uniqueness of the dynamic charging mode calls for further investigation on the extent to which the charging demand in ERS affects power system reliability. As previously discussed, the renewable energy can be used to meet the additional load demand introduced by ERS, but it also poses reliability challenges. In the following, a set of reliability indices, which fully consider the uncertainty of distributed power output and the randomness of EV charging, are proposed. Then, a trip chain based Monte Carlo reliability assessment method is proposed.

### *A. Reliability Indices*

For the power system, three reliability indices are proposed including frequency and duration of annual power shortage. For the EV, four reliability indices related to expected energy consumption and driving distance are proposed to evaluate the reliability of ERS-PSRs.

*1) Reliability Indices for Power System*

1) Loss of load expectation (LOLE): it refers to the annual expected hours of power shortage. LOLE determines the required installed capacity based on the expected capacity during peak periods [35], which is expressed as:

$$LOLE=\sum_{t=0}^{T}T_{loss,t}\Big/\left(60T_m\right) \tag{27}$$

$$T_{loss,t}=\begin{cases}1 & P_{G,t}-P_{load,t}<0\\ 0 & P_{G,t}-P_{load,t}\geq 0\end{cases} \tag{28}$$

where $T$ is the total simulation time (min); $T_{loss,t}$ is the state indicator of the power shortage at time $t$ (min); $T_m$ is the number of simulation years; and $P_{load,t}$ is the system load at time $t$.

Formula (28) compares the load and generation minute by minute, and all minutes with a power shortage are accumulated for the total simulation time.

2) Loss of load probability (LOLP): it implies the probability that the available generation capacity is inadequate for the load demand at the time $t$ [36].

$$LOLP=\frac{\sum_{t=0}^{T}T_{loss,t}}{T} \tag{29}$$

3) Energy not served (ENS): it refers to the discrepancy of energy demand due to power shortage.

$$ENS=\int_0^T\left(P_{G,t}-P_{load,t}\right)T_{loss}\mathrm{d}t \tag{30}$$

*2) Reliability Indices for EV*

1) Expected energy for dynamic charging (EEDC): it refers to the annual expected energy for EVs with dynamic charging.

$$EEDC=\frac{1}{N_{EV}T_m}\sum_{i=1}^{N_{EV,d}}P_{d,i}T_{d,i} \tag{31}$$

where $N_{EV,d}$ is the number of EVs with dynamic charging; $N_{EV}$ is the total number of EVs; $T_{d,i}$ is the duration of dynamic charging for the $i^{\text{th}}$ EV; and $P_{d,i}$ is the power of dynamic charging for the $i^{\text{th}}$ EV.

2) Expected energy for static charging (EESC): it refers to the annual expected energy for EVs with the static charging.

$$EESC = \frac{1}{N_{EV} T_m} \sum_{i=1}^{N_{EV,s}} P_{s,i} T_{s,i} \tag{32}$$

where $N_{ev,s}$ is the number of EVs with static charging; $T_{s,i}$ is the duration of static charging for the $i^{th}$ EV; and $P_{s,i}$ is the power of static charging for the $i^{th}$ EV.

3) Expected energy ratio (EER): it is the ratio of EEDC to the total expected energy.

$$EER = \frac{EEDC}{EEDC + EESC} \times 100\% \tag{33}$$

4) Expected driving distance (EDD): it describes the maximum expected driving distance of EVs in a year.

$$EDD = \frac{EEDC \cdot \alpha_d + EESC \cdot \alpha_s}{EH} \bar{D} \tag{34}$$

where $\alpha_d$ and $\alpha_s$ are the efficiencies of dynamic charging and static charging, respectively; and $\bar{D}$ is the mean driving distance of EVs.

### *B. Trip Chain Based Monte Carlo Reliability Assessment Method*

In this subsection, a simplified trip chain based Monte Carlo reliability assessment method is proposed to evaluate the reliability of ERS-PSRs. The proposed reliability assessment method simulates the charging behavior of each EV in the ERS-PSRs based on the daily travel plan. The daily EV charging load demand and the generated power of power system integrated with renewables can be obtained based on this simulation. The corresponding load can be time-sequentially simulated in minutes when EVs take the daily travel plan as a cycle. The annual simulation time is usually set to be 8760 hours. The loop starts with the first EV for the entire simulation time, followed by the next one, and ends until all EVs are simulated.

The flowchart for the proposed reliability assessment method is illustrated in Fig. 3.

## V. Case Studies

Since the ERS is an emerging concept, there only exist a few pilot projects worldwide, the majority of which are for powering electric trucks using overhead lines. The concept of wireless charging for ERS is an even more novel, making it unfeasible to validate the results on a real system. In this paper, we employ the IEEE Roy Billinton Test System (RBTS), a widely recognized reliability test system, to conduct the simulation experiments [37], [38]. The IEEE RBTS includes 6 buses, 11 generating sets, 9 branches, 2 generating buses, and 4 loads. Its peak power generation is 185 MW [2], [39]. The feeder F4 has 23 load points and 3 types of users: residents, small industries, and businesses. For the ERS-PSRs, the wind power generators and EVs with dynamic charging are integrated.

For the wind power generators, the cut-in, rated, and cut-out wind speeds are 14.4, 45, and 90 km/h, respectively, and the rated power is 3.5 MW. Using the model proposed in Section III-B, the annual predicted wind speed for ERS-PSRs is shown in Fig. 4. Then, the predicted wind power can be obtained by the subsequent calculation. The parameter setting for ERS-PSRs in the simulation are listed in Table II.

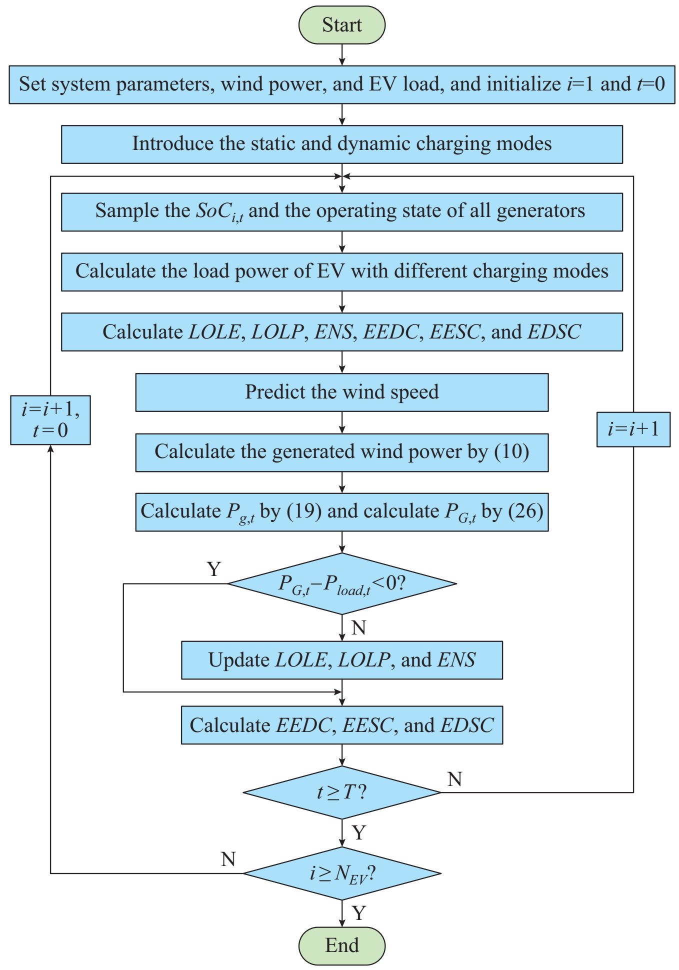


Fig. 3. Flowchart of proposed reliability assessment method.

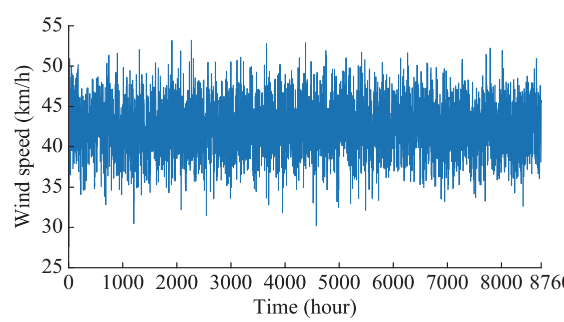


Fig. 4. Annual predicted wind speed for ERS-PSRs.

TABLE II
Parameter Setting for ERS-PSRs in Simulation

| Parameter | Value |
| --- | --- |
| Wind power penetration rate $R_{wind,e}$ (%) | 0 - 30 |
| Ratio of EVs with dynamic charging $R_{EV,d}$ (%) | 0 - 20 |
| The maximum driving distance of EVs (km) | 150 - 300 |
| Ratios of EVs for charging 1, 2, and 3 times per day | 0.6, 0.3, 0.1 |
| Static and dynamic charging power of EV (kW) | 7.36 |
| Static and dynamic charging efficiencies of EV | 0.9, 0.85 |

In January 2023, there were approximately 680000 EVs in the UK [40]. Given that the ERS is a relatively new paradigm, we assume that, only a ratio of 1% EVs, i. e., 680 EVs, are used in the ERS-PSRs for building the load model of EVs.

Figure 5 shows the charging power of EVs when $R_{EV,d}$ is 0, 5%, 10%, and 15%. It can be observed that there are two peak charging periods, i. e., 10: 00 and 20: 00, respectively, during the daily driving of EVs. Additionally, the charging demand is minimal during the period of 12: 00-15: 00 and 01: 00-07: 00, which is primarily attributed to the morning and evening peak periods of urban traffic flow.

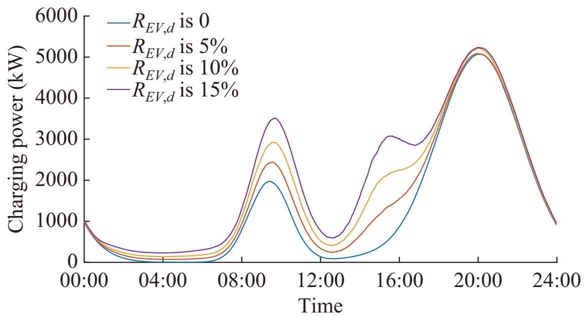


Fig. 5. Charging power of EVs when $R_{EV,d}$ is 0, 5%, 10%, and 15%.

As the ratio of EVs with dynamic charging increases, the load demand of EVs in ERS-PSRs slightly increases in each time period, and a small peak also appears at around 15: 00. Therefore, it can be concluded that after the introduction of dynamic charging for EVs, their load demand will increase, but the flexible charging of ERS-PSRs will theoretically extend the driving distance of EVs.

The power supply-demand relationship is a crucial factor in assessing the reliability of ERS-PSRs. Table III summarizes the reliability indices without considering wind power penetration and EVs with dynamic charging.

TABLE III
RELIABILITY INDICES WITHOUT CONSIDERING WIND POWER PENETRATION AND EVS WITH DYNAMIC CHARGING

| Reliability indices for power system | | | Reliability indices for EV | | | |
|---|---|---|---|---|---|---|
| LOLE (hour) | LOLP ($10^{-3}$) | ENS (MWh) | EEDC (MW) | EESC (MW) | EDDC (%) | EDD (km) |
| 6.975 | 0.798 | 68.803 | 0 | 3.673 | 0 | 20661.74 |

Table III shows that the EDD of each EV is about 20661 km, representing an increase of 35.14% compared with the average distance of pure BEVs (15288 km). A study shows that a typical Tesla Model S covers about 19942 km per year, as measured from a sample of 887 EVs [41]. The dynamic charging technology leads to the longest driving distance of EVs.

1) Impact of wind power penetration and EVs with dynamic charging on reliability indices for power system

In this case, the reliability indices for power system with different $R_{wind,e}$ and $R_{EV,d}$ are given in Table IV. Figure 6 shows the value of LOCE in ERS-PSRs to analyze the reliability. It is evident from Table IV that the annual power shortage becomes more frequent as $R_{wind,e}$ and $R_{EV,d}$ increase in the ERS-PSRs. One of the reasons is the introduction of dynamic charging for EVs, which extends their driving distance but results in a significant increase of load demand of EVs, leading to a more serious power shortage. As shown in Fig. 6, when $R_{wind,e}$ increases, the value of LOLE grows rapidly. Furthermore, it can be noted from Table IV that the power shortage increases by about 1 MW annually with every 5% of EVs retrofitted to accept the dynamic charging mode.

TABLE IV
RELIABILITY INDICES FOR POWER SYSTEM WITH DIFFERENT $R_{wind,e}$ AND $R_{EV,d}$

| $R_{wind,e}$ (%) | $R_{EV,d}$ (%) | LOLE (hour) | LOLP ($10^{-3}$) | ENS (MWh) |
|---|---|---|---|---|
| 10 | 0 | 6.537 | 0.748 | 56.090 |
| | 5 | 6.595 | 0.754 | 56.663 |
| | 10 | 6.935 | 0.793 | 61.416 |
| | 15 | 7.120 | 0.815 | 62.646 |
| 20 | 0 | 4.450 | 0.510 | 33.797 |
| | 5 | 4.650 | 0.532 | 34.635 |
| | 10 | 4.760 | 0.544 | 36.191 |
| | 15 | 4.920 | 0.563 | 36.924 |
| 30 | 0 | 17.052 | 1.951 | 125.075 |
| | 5 | 18.232 | 2.087 | 135.667 |
| | 10 | 18.920 | 2.165 | 142.352 |
| | 15 | 19.410 | 2.222 | 142.612 |
| 40 | 0 | 33.397 | 3.823 | 225.644 |
| | 5 | 34.670 | 3.968 | 234.382 |
| | 10 | 36.290 | 4.154 | 246.339 |
| | 15 | 39.440 | 4.514 | 258.565 |

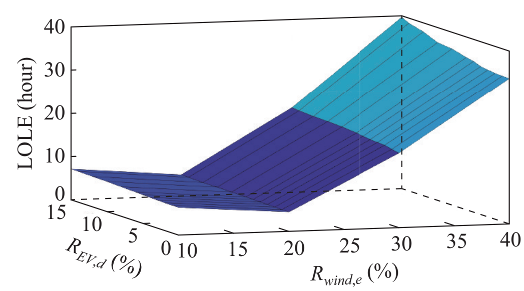


Fig. 6. Value of LOLE in ERS-PSRs.

As $R_{wind,e}$ increases slightly (10%), it can be observed that the power shortage almost remains unchanged. The LOLE still maintains at about 6-7 hours. The reason is that, the deficit caused by conventional power plants can be reduced when wind power generators replace failed generation during peak periods. When $R_{wind,e}$ is 20%, the power shortage is the lowest. As $R_{wind,e}$ continues to increase, the power shortage becomes more frequent. Therefore, a value of 20% for $R_{wind,e}$ appears to be the optimal solution for achieving carbon reduction in the ERS-PSRs under the investigation in this study.

2) Impact of EVs with dynamic charging on reliability indices for EVs

The reliability indices for EVs with different $R_{EV,d}$ are given in Table V.

TABLE V
RELIABILITY INDICES FOR EVS WITH DIFFERENT $R_{EV,d}$

| $R_{EV,d}$ (%) | EEDC (MWh) | EESC (MWh) | EDD (km) | EDDC (%) |
|---|---|---|---|---|
| 0 | 0 | 3.6732 | 20661.74 | 0 |
| 5 | 0.2732 | 3.6564 | 22017.99 | 6.95 |
| 10 | 0.5487 | 3.6611 | 23542.40 | 13.03 |
| 15 | 0.8407 | 3.6653 | 25083.53 | 18.65 |

It can be observed in Table V that when $R_{EV,d}$ increases from 0 to 15%, the EEDC increases, while the EESC remains relatively unchanged at around 3.66 MWh. Meanwhile, the EDD increases from 20661.74 to 25083.53 km, which is an increase of 18.6%. It can be concluded that a higher rate of EVs with dynamic charging will result in longer driving distances for EVs, as well as higher costs and longer load construction time.

3) Impact of additional wind power

In addition to the increasing number of EVs, the introduction of dynamic charging mode will also introduce additional uncertain loads and thus impact the reliability of power system. To fill the power gap caused by EVs, this part considers the impact of additional wind power $R'_{wind,e}$ on the reliability indices for the power system, as given in Table VI.

TABLE VI
RELIABILITY INDICES FOR POWER SYSTEM WITH DIFFERENT $R'_{wind,e}$

| $R'_{wind,e}$ (%) | $R_{EV,d}$ (%) | LOLE (hour) | LOLP ($10^{-4}$) | ENS (MWh) |
|---|---|---|---|---|
| 0 | 0 | 6.757 | 7.735 | 66.410 |
| | 5 | 6.984 | 7.995 | 67.248 |
| | 10 | 7.271 | 8.323 | 68.586 |
| | 15 | 7.642 | 8.748 | 74.148 |
| 4 | 0 | 3.817 | 4.370 | 37.451 |
| | 5 | 3.991 | 4.568 | 37.486 |
| | 10 | 4.416 | 4.746 | 37.585 |
| | 15 | 4.391 | 5.026 | 41.541 |
| 8 | 0 | 1.635 | 1.872 | 14.230 |
| | 5 | 1.668 | 1.910 | 13.909 |
| | 10 | 1.737 | 1.989 | 15.003 |
| | 15 | 1.924 | 2.202 | 16.213 |

It is evident that as $R'_{wind,e}$ increases, the power shortage decreases significantly and the LOLP also decreases. The additional wind power clearly improves the reliability indices for the power system. Obviously, when $R_{EV,d}$ is 5%, the 1 MW additional wind power can maintain the ENS and LOLE at a comparable level to the original system, at around 66 MWh and 6 hour, respectively. It can be summarized from Table VI that the current power system can accommodate about 10%-15% of EVs with dynamic charging without significant changes.

As discussed early, with the development of electric roads, it is clear that simply increasing the penetration rate of renewable energy is not enough to fill the power supply gap caused by dynamic charging. Therefore, adding more wind power may be a better solution to maintain reliable operation of the power system. It is also known that for every 2% additional wind power, the LOLE decreases by approximately half, and the annual power shortage decreases about 45%. The additional wind power can be planned based on different operating requirements for further analysis.

4) Impact of BESS

In the aforementioned analysis, EVs are only considered as pure loads. However, in ERSs, EVs can serve not only as loads but also as BESS.

Based on the optimal wind power penetration rate of 20%, this paper conducts a reliability analysis of the power system with BESS, and the results are summarized in Table VII.

TABLE VII
RELIABILITY INDICES FOR POWER SYSTEM WITH BESS

| $R_{ev,d}$ (%) | LOLE (hour) | LOLP ($10^{-4}$) | ENS (MWh) |
|---|---|---|---|
| 0 | 4.360 | 4.990 | 33.321 |
| 5 | 4.595 | 5.259 | 34.251 |
| 10 | 4.760 | 5.345 | 35.768 |
| 15 | 4.852 | 5.554 | 36.487 |

As compared with Table V, it is evident that when the power system incorporates BESS, the ENS slightly increases while the LOLE remains almost unchanged. It can be concluded that when EVs are regarded as BESSs, they can alleviate some of the energy supply pressure, thereby achieving peak shaving and valley filling, and leading to better system performance.

## VI. CONCLUSION

The introduction of EVs with dynamic charging in the ERS-PSRs can bring several potential benefits, including travel range extension and emission reduction. However, the increased load demand of EVs presents unknown reliability issues for the power system. The key contributions and findings of this paper are summarized as follows.

1) A range of charging scenarios and environments for EVs are modeled and several quantitative reliability indices are proposed. To analyze the reliability of ERS-PSRs in the context of EVs with dynamic charging, the charging modes and daily trip trains of EVs are designed, and a trip chain based Monte Carlo reliability assessment method for ERS-PSRs is developed.

2) The impacts of the wind power penetration rate, the rate of EVs with dynamic charging, and additional wind power on the reliability of ERS-PSRs are all analyzed in detail. Furthermore, the impact of taking EVs as BESSs on the reliability of ERS-PSRs is also assessed.

3) The results from the case studies in the IEEE RBTS have confirmed that integrating EVs with dynamic charging into the ERS-PSRs can significantly increase the EDD of EVs. When the wind power penetration rate accounts for 20%, the system can maintain at a more reliable state while reducing carbon emissions. To bridge the power supply gap caused by EV charging, an additional 5% wind power is suggested for the stable system operation.

With the future roll-out of the ERS and decarbonized road vehicles, the coupling effects of the road traffic network and the power grid will become even more prominent and complex. We will continue to engage with different stakeholders to collect more data to meet the power supply challenges of ERSs.

## References


[1] M. Shen, W. Huang, M. Chen *et al*., "(Micro)plastic crisis: un-ignorable contribution to global greenhouse gas emissions and climate change," *Journal of Cleaner Production*, vol. 254, p. 120138, May 2020.

[2] W. Zuo and K. Li, "Reliability assessment of integrated power and road system for decarbonizing heavy-duty vehicles," *Energies*, vol. 17, no. 4, p. 934, Feb. 2024.

[3] I. Tiseo. (2024, May). Distribution of carbon dioxide emissions produced by the transportation sector worldwide in 2020, by subsector. 2021. [Online]. Available: https://www. statista. com/statistics/1185535/transport-carbon-carbon-dioxide-emissions-breakdown/

[4] IEA. Transport: "Improving the sustainability of passenger and freight transport," IEA Paris, France, Tech. Rep., 2021.

[5] X. Wang, M. Shahidehpour, C. Jiang *et al*., "Coordinated planning strategy for electric vehicle charging stations and coupled traffic-electric networks," *IEEE Transactions on Power Systems*, vol. 34, no. 1, pp. 268-279, Jan. 2019.

[6] SMMT. (2024, Feb.). Delivering consumer-centric charging infrastructure for zero emission mobility. [Online]. Available: chrome-extension: //efaidnbmnnnibpcajpcglclefindmkaj/https://www. smmt. co. uk/wp-content/uploads/SMMT-EV-Infrastructure-Position-Paper-FINAL.pdf

[7] E. M. Bibra, E. Connelly, S. Dhir *et al*. (2024, Feb.). Global EV outlook 2022: securing supplies for an electric future. [Online]. Available: https://www.iea.org/reports/global-ev-outlook-2022

[8] J. Wishart. (2024, Feb.). Fuel cells vs batteries in the automotive sector. [Online]. Available: https://www. researchgate. net/publication/311210193

[9] D. Bateman, D. Leal, S. Reeves *et al*. (2023, Aug.). Electric road systems: a solution for the future. [Online]. Available: https://trid.trb.org/view/1570673

[10] L. Nordin, F. Hellman, A. Genell *et al*. (2022, Aug.). Environmental impact of electric road systems: a compilation of the literature review of work package 2 in the FOI-platform for electrified roads. [Online]. Available: https://www.diva-portal.org/smash/get/diva2:1445414/FULLTEXT03.pdf

[11] W. Zuo and K. Li, "Electrical vehicle charging strategy for electric road systems considering V2G technology," in *Proceedings of 2023 IEEE International Conference on Energy Technologies for Future Grids* (*ETFG*), Wollongong, Australia, Dec. 2023, pp. 1-5.

[12] J. Schulte and H. Ny, "Electric road systems: strategic stepping stone on the way towards sustainable freight transport?" *Sustainability*, vol. 10, no. 4, p. 1148, Apr. 2018.

[13] S. Tongur, "Preparing for takeoff: analyzing the development of electric road systems from a business model perspective," Ph.D. dissertation, KTH Royal Institute of Technology, 2018.

[14] J. Huh and C. T. Rim. (2023, Feb.). KAIST wireless electric vehicles – OLEV. [Online]. Available: https://www. sae. org/publications/technical-papers/content/2011-39-7263/

[15] Electreon. (2023, Feb.). Possibilities for large-scale electric road development. [Online]. Available: https://electreon.com/projects/gotland.

[16] A. Boone. (2023, Feb.). Simulation of short-term wind speed forecast errors using a multi-variate ARMA (1, 1) time-series model. [Online]. Available: https://www. diva-portal. org/smash/get/diva2: 604579/FULLTEXT01.pdf

[17] C. Yu, Y. Xue, F. Wen *et al*., "Risk assessment of wind power prediction errors," *Automation of Electric Power Systems*, vol. 39, no. 7, pp. 52-58, Jan. 2015.

[18] Y. Chen, Z. Tian, C. Roberts *et al*., "Reliability and life evaluation of a DC traction power supply system considering load characteristics," *IEEE Transactions on Transportation Electrification*, vol. 7, no. 3, pp. 958-968, Sept. 2021.

[19] D. Feng, S. Lin, Q. Yang *et al*., "Reliability evaluation for traction power supply system of high-speed railway considering relay protection," *IEEE Transactions on Transportation Electrification*, vol. 5, no. 1, pp. 285-298, Mar. 2019.

[20] X. Wang, M. Shahidehpour, C. Jiang *et al*., "Resilience enhancement strategies for power distribution network coupled with urban transportation system," *IEEE Transactions on Smart Grid*, vol. 10, no. 4, pp. 4068-4079, Jul. 2019.

[21] P. Gomes and R. Castro, "Wind speed and wind power forecasting using statistical models: autoregressive moving average (ARMA) and artificial neural networks (ANN)," *International Journal of Sustainable Energy Development*, vol. 1, no. 2, pp. 41-50, Dec. 2012.

[22] R. Karki, P. Hu, and R. Billinton, "A simplified wind power generation model for reliability evaluation," *IEEE Transactions on Energy Conversion*, vol. 21, no. 2, pp. 533-540, Jun. 2006.

[23] W. Wangdee and R. Billinton, "Considering load-carrying capability and wind speed correlation of WECS in generation adequacy assessment," *IEEE Transactions on Energy Conversion*, vol. 21, no. 3, pp. 734-741, Sept. 2006.

[24] C. Carrillo, A. F. O. Montaño, J. Cidrás *et al*., "Review of power curve modelling for wind turbines," *Renewable and Sustainable Energy Reviews*, vol. 21, pp. 572-581, May 2013.

[25] M. Lydia, S. S. Kumar, A. I. Selvakumar *et al*., "A comprehensive review on wind turbine power curve modeling techniques," *Renewable and Sustainable Energy Reviews*, vol. 30, pp. 452-460, Feb. 2014.

[26] M. Shepero, J. Munkhammar, J. Widén *et al*., "Modeling of photovoltaic power generation and electric vehicles charging on city-scale: a review," *Renewable and Sustainable Energy Reviews*, vol. 89, pp. 61-71, Jun. 2018.

[27] K. Qian, C. Zhou, M. Allan *et al*., "Modeling of load demand due to EV battery charging in distribution systems," *IEEE Transactions on Power Systems*, vol. 26, no. 2, pp. 802-810, May 2011.

[28] S. Tao, K. Liao, X. Xiao *et al*., "Charging demand for electric vehicle based on stochastic analysis of trip chain," *IET Generation*, *Transmission & Distribution*, vol. 10, no. 11, pp. 2689-2698, Aug. 2016.

[29] F. Primerano, M. A. P. Taylor, L. Pitaksringkarn *et al*., "Defining and understanding trip chaining behaviour," *Transportation*, vol. 35, no. 1, pp. 55-72, Jan. 2008.

[30] H. Zhang, C. J. R. Sheppard, T. E. Lipman *et al*., "Joint fleet sizing and charging system planning for autonomous electric vehicles," *IEEE Transactions on Intelligent Transportation Systems*, vol. 21, no. 11, pp. 4725-4738, Nov. 2020.

[31] J. Lin, L. Cheng, Y. Chang *et al*., "Reliability based power systems planning and operation with wind power integration: a review to models, algorithms and applications," *Renewable and Sustainable Energy Reviews*, vol. 31, pp. 921-934, Mar. 2014.

[32] J. Wang, Q. Zhou, and X. Zhang, "Wind power forecasting based on time series ARMA model," *IOP Conference Series: Earth and Environmental Science*, vol. 199, p. 022015, Dec. 2018.

[33] C. Eisenhut, F. Krug, C. Schram *et al*., "Wind-turbine model for system simulations near cut-in wind speed," *IEEE Transactions on Energy Conversion*, vol. 22, no. 2, pp. 414-420, Jun. 2007.

[34] W. Jiang, Z. Yan, and D. Feng, "A review on reliability assessment for wind power," *Renewable and Sustainable Energy Reviews*, vol. 13, no. 9, pp. 2485-2494, Dec. 2009.

[35] R. N. Allan. *Reliability Evaluation of Power Systems*. Berlin: Springer Science Business Media, 2013.

[36] B. Hu, C. Pan, C. Shao *et al*., "Decision-dependent uncertainty modeling in power system operational reliability evaluations," *IEEE Transactions on Power Systems*, vol. 36, no. 6, pp. 5708-5721, Nov. 2021.

[37] R. Billinton and R. N. Allan, *Reliability Evaluation of Engineering Systems*. Boston: Springer US, 1992.

[38] W. Li, *Reliability Assessment of Electric Power Systems Using Monte Carlo Methods*. Berlin: Springer Science & Business Media, 2013.

[39] S. Pulendran and J. E. Tate, "Energy storage system control for prevention of transient under-frequency load shedding," *IEEE Transactions on Smart Grid*, vol. 8, no. 2, pp. 927-936, Mar. 2017.

[40] Z. MAP. (2023, Feb.). Electric vehicle market statistics 2023. [Online]. Available: https://www.zap-map.com/ev-market-statistics

[41] M. Research. (2023, Feb.). The average electric car is driven 9,500 miles a year. [Online]. Available: https://www. motoringresearch. com/car-news/ average-electric-car-driven-9500-year


**Wei Zuo** received B.Eng. degree in electrical engineering from University of South China, Hengyang, China, in 2018, and the M.Sc. degree in electrical engineering from Hunan University, Changsha, China, in 2020. She is currently pursuing the Ph.D. degree in electronic/electrical engineering in University of Leeds, Leeds, UK. Her research interests include reliability analysis of electrical railway traction power supply system and electric road system.

**Kang Li** received the B.Sc. degree in industrial automation from Xiangtan University, Xiangtan, China, in 1989, the M.Sc. degree in control theory and applications from Harbin Institute of Technology, Harbin, China, in 1992, and the Ph.D. degree in control theory and applications from Shanghai Jiao Tong University, Shanghai, China, in 1995. He also received D.Sc. degree in engineering from Queen's University Belfast, Belfast, UK, in 2015. He currently holds the Chair of Smart Energy Systems and is the Director of the Institute of Communication and Power Networks, School of Electronic and Electrical Engineering, University of Leeds, Leeds, UK. His research interests include nonlinear system modelling, identification, and control, and machine learning, with substantial applications to energy and power system, smart grid, transport decarbonization, and energy management in energy intensive manufacturing processes.

**Jihai Zhong** received the B.S. degree in electronic information engineering from Guangdong University of Petrochemical and Technology, Maoming, China, in 2019, and the M.S. degree in communication and signal processing from University of Leeds, Leeds, UK, in 2020, respectively. He is currently pursuing the Ph.D. degree with the School of Electronic and Electrical Engineering, University of Leeds. His research interests include handover in wireless communication, drones assisted network, and cellular radio.